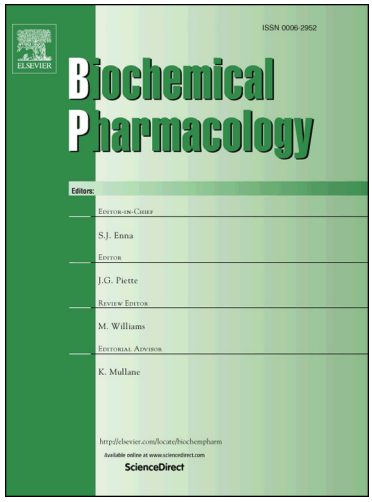

Loperamide overcomes the resistance of colon cancer cells to bortezomib by inducing CHOP-mediated paraptosis-like cell death

In Young Kim, Min June Shim, Dong Min Lee, A Reum Lee, Mi Ae Kim, Mi Jin Yoon, Mi Ri Kwon, Hae In Lee, Min Ji Seo, Yong Won Choi, Kyeong Sook Choi

PII: S0006-2952(18)30505-7
DOI: https://doi.org/10.1016/j.bcp.2018.12.006
Reference: BCP 13370

To appear in: *Biochemical Pharmacology*

Received Date: 16 October 2018
Accepted Date: 6 December 2018

Please cite this article as: I. Young Kim, M. June Shim, D. Min Lee, A. Reum Lee, M. Ae Kim, M. Jin Yoon, M. Ri Kwon, H. In Lee, M. Ji Seo, Y. Won Choi, K. Sook Choi, Loperamide overcomes the resistance of colon cancer cells to bortezomib by inducing CHOP-mediated paraptosis-like cell death, *Biochemical Pharmacology* (2018), doi: https://doi.org/10.1016/j.bcp.2018.12.006

Loperamide overcomes the resistance of colon cancer cells to bortezomib by inducing CHOP-mediated paraptosis-like cell death

In Young Kim[1], Min June Shim[1,2], Dong Min Lee[1,2], A Reum Lee[1,2], Mi Ae Kim[1,2], Mi Jin Yoon[1], Mi Ri Kwon[1,2], Hae In Lee[1,2], Min Ji Seo[1,2], Yong Won Choi[3], Kyeong Sook Choi[1,2]

[1]Department of Biochemistry and Molecular Biology, Ajou University, Suwon 16499 Korea

[2]Department of Biomedical Science, Ajou University Graduate School of Medicine, Suwon 16499 Korea

[3]Department of Hematology-Oncology, Ajou University School of Medicine, Suwon 16499, Korea

Corresponding Author: Kyeong Sook Choi, Ph.D.

Department of of Biochemistry

Ajou University School of Medicine

Department of Biomedical Sciences, Ajou Graduate School

164, World cup-ro, Yeongtong-gu, Suwon, 16499, Korea

E-mail: kschoi@ajou.ac.kr

Phone: 82-31-219-4552

Fax: 82-31-219-5059

ABSTRACT

Although the proteasome inhibitor (PI) bortezomib (Btz) is in current clinical use as a front-line treatment for multiple myeloma, its clinical efficacy in solid tumors has not been satisfactory. Here, we show that loperamide (Lop), an antidiarrheal drug, effectively sensitizes various colon cancer cells, but not normal epithelial cells, to PI-mediated cell death. We report that combined treatment with Btz and Lop induces paraptosis-like cell death accompanied by severe endoplasmic reticulum (ER)-derived vacuolation. Furthermore, Lop potentiates Btz-mediated ER stress and ER dilation due to misfolded protein accumulation and Ca^{2+} imbalance, leading to CHOP upregulation and subsequent paraptosis-like cell death. Taken together, our results show for the first time that a combined regimen of PI and Lop may provide an effective and safe therapeutic strategy against solid tumors, including colon cancer, by enhancing the sensitivity to PIs and reducing the side effects of such treatment.

Keywords: bortezomib, loperamide, paraptosis-like cell death, ER stress, CHOP

1. Introduction

As many as one third of newly synthesized proteins are degraded within minutes by proteasome [1]. The ubiquitin proteasome system (UPS) is a central component of the cellular protein degradation machinery; it performs essential functions in homeostasis, such as by preventing the accumulation of misfolded or deleterious proteins. Cancer cells produce proteins that promote cell survival and proliferation and/or inhibit cell death mechanisms. Deregulation of the UPS can enhance or reduce the degradation of key targets that contribute to oncopathogenesis [2], prompting researcher to perform preclinical testing of proteasome inhibitors as a means to shift this fine equilibrium towards cell death [2, 3]. Among the PIs, inhibitors of the 20S proteolytic core of the proteasome have been the most extensively studied; three of these agents—bortezomib (Btz), carfilzomib (Cfz), and ixazomib (Ixz)—are currently approved for the treatment of multiple myeloma (MM) and mantle-cell lymphoma (MCL) [4, 5]. Btz sensitizes MM cells to the effects of conventional chemotherapy with major response rates of over 50% observed in a relapse setting [6]. In addition, PIs have been the subject of continuing interest for the treatment of solid tumors [7,8]. However, Btz has a number of side effects, including thrombocytopenia, peripheral neuropathy, nausea, and diarrhea [6,8]. Additionally, both primary (or innate) and secondary (or acquired) resistance mechanisms increasingly compromise the effectiveness of PI therapy [9]. The clinical efficacy of Btz or Cfz (a second-generation PI) mono-treatment has proven limited in solid tumors [10,11]. The concentrations of these PIs that are clinically relevant in hematopoietic tumors are not active in solid tumors of different organs, suggesting that stronger inhibition of the proteasome may be necessary for efficacy in such tumors. However, simple elevation of the drug concentration may cause side effects. Thus, we urgently need to design safer and more effective PI-based cancer strategies.

Discovery of drugs that can enhance the efficacy of PIs and subsequent optimization of combination regimens might help broaden the applicability of PIs to other hematological malignancies as well as solid tumors. It would further benefit cancer patients, if the co-treated PI sensitizer could ameliorate the side effects of the PI. Diarrhea is a side effect of Btz and Loperamide (Lop) is clinically used to reduce the side effects experienced by PI-treated cancer patients with complications, including diarrhea [8]. In addition, the malignant proliferation of plasma cells produces skeletal destruction that leads to bone pain in MM [12], and Lop has been shown to exhibit analgesic effects in animal models of pain, including a bone cancer pain model [13,14].

In the present study, we show for the first time that Lop can effectively sensitize various colon cancer cells, but not normal colon cells, to the anticancer activities of PIs (including Btz, Cfz, and Ixz). Additionally, Lop sensitizes various other types of cancer cells to Btz-mediated cell death. Interestingly, we find that a combination of Btz and Lop (Btz/Lop) kills colon cancer cells primarily by inducing paraptosis-like cell death accompanied by severe endoplasmic reticulum (ER)-derived vacuolation, rather than through apoptosis. Paraptosis is a programmed cell death mode characterized by dilation of the ER and/or mitochondria [16]. It lacks apoptotic features, including chromatin condensation, DNA fragmentation, apoptotic body formation, and caspase dependency, and is known to require *de novo* protein synthesis [15,16]. Although the molecular basis of paraptosis remains to be clarified, the process is known to be associated with the perturbation of cellular proteostasis via proteasomal inhibition [17-19] and disruption of Ca^{2+} homeostasis [18,20,21]. Here, we show that Lop effectively enhances Btz-mediated ER stress and dilation of the ER related to accumulation of misfolded proteins and increased Ca^{2+} levels, and that this contributes to CHOP upregulation and subsequent paraptosis-like cell death in colon cancer cells. Our findings suggest that a combined regimen of Btz and Lop could improve the efficacy and safety of PI-

based therapy for the treatment of solid tumors, including colon cancer.

2. Materials and Methods

2.1. Chemicals and antibodies

Chemicals and reagents were obtained as follows: Btz from Selleckchem (Houston, TX, USA); Lop from Tocris (Ellisville, MO, USA). Ixz (MLN9708) from Cayman Chemical (Ann Arbor, MI, USA); Ru360 from Calbiochem (EDM Millipore Corp., Billerica, MA, USA); MitoTracker-Red (MTR), propidium iodide (PI), Fluo-3-AM, Rhod-2-AM, and 4',6-diamidino-2-phenylindole (DAPI) from Molecular Probes (Eugene, OR, USA); z-VAD-fmk from R&D Systems (Minneapolis, MN, USA); and Carfilzomib (Cfz), 3-methyladenine (3-MA), bafilomycin A1 (Baf A), chloroquine (CQ), 1,2-bis(2-aminophenoxy)ethane-N,N,N',N'-tetraacetic acid (BAPTA), 2,3-bis(2-aminophenoxy)ethane-N,N,N',N'-tetraacetic acid tetrakis(acetoxymethyl ester) (BAPTA-AM), ethylene-bis(oxyehylenenitrilo)tetraacetic acid (EGTA), ruthenium red, crystal violet and cycloheximide (CHX) from Sigma-Aldrich (St. Louis, MO, USA). The following primary antibodies were used: α-tubulin (sc-32293) and ubiquitin (sc-8017) from Santa Cruz Biotechnology (Santa Cruz, CA, USA); CHOP/GADD153 (#2895), PERK (#5683), and IRE1 (#3294) from Cell Signaling Technology (Danvers, MA, USA); caspase-3 (ADI-AAP-113) from Enzo Life Sciences (Farmingdale, NY, USA); BAP31 (ab37120) and poly (ADP-ribose) polymerase (PARP; ab32071) from Abcam (Cambridge, UK). The secondary antibodies, including rabbit IgG HRP (G-21234) and mouse IgG HRP (G-21040), were obtained from Molecular Probes.

2.2. Cell culture

DLD-1, SW-480, SW-620, HCT116 (all from colon cancers), HeLa (cervical cancer), Caki-1 (kidney cancer), T98G (glioblastoma), MDA-MB 435S (breast cancer), and CCD-112CoN (normal colon) cells were purchased from the American Type Culture Collection (ATCC, Manassas, VA, USA). SNU-449 (hepatocellular carcinoma) cells were obtained from the Korean Cell Line Bank (KCLB, Seoul, Korea). DLD-1, SW-480, SW-620, HCT116, HeLa, Caki-1, T98G, and MDA-MB 435S cells were cultured in DMEM supplemented with 10% fetal bovine serum (FBS) and 1% antibiotics (GIBCO-BRL, Grand Island, NY, USA). SNU-449 cells were cultured in RPMI-1640 medium supplemented with 10% FBS and 1% antibiotics. CCD-112CoN cells were maintained in MEM supplemented with 10% FBS and 1% antibiotics. Cells were incubated in 5% CO_2 at 37°C.

2.3. Cell viability assay

Cells were cultured in 48-well plates and treated as indicated. The cells were then fixed with methanol/acetone (1:1) at -20°C for 5 min, washed three times with PBS, and stained with propidium iodide (PI; final concentration, 1 μg/ml) at room temperature for 10 min. The plates were imaged on an IncuCyte device (Essen Bioscience, Ann Arbor, MI, USA) and analyzed using the IncuCyte ZOOM 2016B software. The processing definition of the IncuCyte program was set to recognize attached (live) cells by their red-stained nuclei. The percentage of live cells was normalized to that found in untreated control cultures (100%).

2.4. Clonogenic assay

To determine long-term anticancer effects, DLD-1 cells seeded on 12-well plates were treated with 40 nM Btz and/or 20 μM Lop for 4 h. The medium was then replaced with fresh medium, the cells were allowed to grow for 8 days to form colonies, and the colonies were stained with 0.5% crystal violet.

2.5. Morphological examination of the ER and mitochondria

To establish stable cell lines expressing fluorescence specifically in the ER, DLD-1 cells were transfected with the pEYFP-ER vector (Clontech, Mountain View, CA, USA). Stable cell lines expressing pEYFP-ER (YFP-ER) were selected with fresh medium containing 500 μg/ml G418 (Calbiochem). After treatments, YFP-ER cells were stained with 100 nM Mito-Tracker Red (MTR) for 15 min and the morphological changes of the ER and mitochondria were observed under a K1-Fluo confocal laser-scanning microscope (Nanoscope Systems. Daejeon, Korea).

2.6. Cell cycle analysis

After treatments, cells were trypsinized, washed with PBS-EDTA, and fixed in 70% (v/v) ethanol. DNA contents were assessed by propidium iodide (PI) staining followed by analysis on a FACSAria™ III (BD Biosciences, San Jose, CA, USA). The data were analyzed using the FACSDiva software (BD Biosciences).

2.7. Immunoblot analyses

Immunoblot analysis was performed as described previously [17]. The fold change of each target protein level compared to α-tubulin was determined by densitometric analysis.

2.8. Immunofluorescence microscopy

After treatments, the cells were fixed with acetone/methanol (1:1) for 5 min at -20°C and blocked in 5% BSA in PBS for 30 min. Fixed cells were incubated overnight at 4°C with primary antibodies diluted in PBS [anti-ubiquitin (1:500, mouse, Santa Cruz Biotechnology), anti-CHOP (1:500, mouse, Cell Signaling Technology) and/or anti-BAP31 (1:500, rabbit,

Abcam)], washed three times in PBS, and incubated for 1 h at room temperature with anti-mouse or anti-rabbit Alexa Fluor 488 or 594 (1:1000, Molecular Probes). Slides were mounted with ProLong Gold antifade mounting reagent (Molecular Probes) and cell staining was visualized with the K1-Fluo confocal laser scanning microscope.

2.9. Transmission electron microscopy

Cells were pre-fixed in Karnovsky's solution (1% paraformaldehyde, 2% glutaraldehyde, 2 mM calcium chloride, 0.1 M cacodylate buffer, pH 7.4) for 2 h and washed with cacodylate buffer. Post-fixing was carried out in 1% osmium tetroxide and 1.5% potassium ferrocyanide for 1 h. After dehydration with 50-100% alcohol, the cells were embedded in Poly/Bed 812 resin (Pelco, Redding, CA, USA), polymerized, and observed under an electron microscope (EM 902A, Carl Zeiss, Oberkochen, Germany).

2.10. Small interfering RNA- or small hairpin RNA-mediated knockdown of proteins

The siRNA duplexes used in this study were purchased from Invitrogen (Carlsbad, CA, USA) and had the following sequences: CHOP (NCBI accession no. NM_004083, 5'-GAGCUCUGAUUGACCGAAUGGUGAA-3'). The Negative Universal Control siRNA (Invitrogen) was used as the control. The pairs of siRNA oligonucleotides were annealed and transfected to cells using the RNAiMAX reagent (Invitrogen), according to the manufacturer's instructions. To confirm successful siRNA-mediated knockdown, Western blotting of the proteins of interest was performed.

2.11. Measurement of cytosolic and mitochondrial Ca^{2+} levels

To measure cytosolic Ca^{2+} levels ($[Ca^{2+}]_c$), treated cells were incubated with 1 μM Fluo-3-AM at 37 °C for 20 min, washed with HBSS (without Ca^{2+} or Mg^{2+}), and analyzed

immediately by flow cytometry using a FACSAria™ III, or visualized by Axiovert 200M fluorescence microscopy (Carl Zeiss). To measure mitochondrial Ca^{2+} levels ($[Ca^{2+}]_{mt}$), treated cells were incubated with 1 μM Rhod-2-AM at 4 °C for 30 min, washed with HBSS (without Ca^{2+} or Mg^{2+}), further incubated with HBSS at 37 °C for 20 min, and then analyzed by flow cytometry.

2.12. Live-cell imaging

DLD-1 cells were seeded to a 12-well plate (BD Biosciences) and treated with 40 nM Btz and/or 20 μM Lop for 16 h. Phase contrast time-lapse images were analyzed on a Zeiss Cell Observer System. Cells were incubated at 37°C in humidified atmosphere containing 5% CO_2. Images were collected with an EC-Neofluar 20X/0.4 and AxioCam MRm (Carl Zeiss) every 30 min and processed using the AxioVision software.

2.13. Isobologram analysis

To determine how the combinations of PIs and Lop affected the cancer cell lines, dose-dependent effects were determined for each compound alone and with a fixed concentration of the other co-treated agent. The interactions of the PIs and Lop were quantified by determining the combination index (CI), in accordance with the following classic isobologram equation [22]: $CI = (D)_1/(Dx)_1 + (D)_2/(Dx)_2$, where $(Dx)_1$ and $(Dx)_2$ indicate the individual doses of Btz and Lop, respectively, required to produce an effect, and $(D)_1$ and $(D)_2$ are the doses of Btz and Lop, respectively, that produce the same effect when applied in combination. From this analysis, the combined effects of the two drugs can be summarized as follows: $CI < 1$ indicates synergism; $CI = 1$ indicates summation (additive and zero interaction); and $CI > 1$ indicates antagonism.

2.14. Statistical analysis

All data are presented as the mean ± SD (standard deviation) from at least three separate experiments. The GraphPad Prism software (GraphPad Software Inc, San Diego, CA, USA) was used to perform the statistical analyses. Normality of data was assessed by the Kolmogorov-Smirnov test and equal variance was assessed using Bartlett's test. For a normal distribution, statistical differences were determined using analysis of variance (ANOVA) followed by Bonferroni's multiple comparison test.

3. Results

3.1. Loperamide effectively enhances cell death in colon cancer cells treated with proteasome inhibitors

In an attempt to identify a sensitizer that can effectively overcome the resistance of cancer cells to PI, we investigated whether Lop, an antidiarrheal drug, could sensitize colon cancer cells to various PIs. Treatment with Lop up to 30 μM was not cytotoxic toward various colon cancer cells, including DLD-1, SW-480, HCT116, and SW-620 cells (Figure 1A). Among the tested cells, DLD-1 cells were the most resistant to Btz, exhibiting no significant change in viability when treated with 60 nM Btz. Conversely, SW-620 cells were relatively sensitive to Btz, with 15 nM Btz decreasing viability to ~60% of the control level. Importantly, Lop dose-dependently enhanced cell death when combined with subtoxic doses of Btz in all tested cancer cell lines. Isobologram analysis revealed that Lop and Btz synergistically induced cell death in these cells (Figure 1B). Colony-forming assays demonstrated that the combination of Btz with Lop (Btz/Lop), but not either mono-treatment, markedly reduced the clonogenicity of DLD-1 cells (Figure 1C). Taken together, these results indicate that Lop effectively overcomes Btz resistance in many colon cancer cell lines. To test whether Lop demonstrates

a sensitizing effect on cancer cells treated with other PIs, we treated DLD-1 or HCT 116 cells with subtoxic doses of Lop together with the FDA-approved PIs, carfilzomib (Cfz) or ixazomib (Ixz). Indeed, Lop and the tested PIs dose-dependently and synergistically induced cell death in these cancer cells (Figure 1D and 1E), suggesting that Lop may act as an effective sensitizer of various PIs. Interestingly, CCD-112CoN cells (a normal colon cell line) appeared quite resistant to the combined effects of Btz, Cfz, or Ixz plus Lop at concentrations that demonstrated synergistic effects in DLD-1 or HCT116 cells (Figure 1F). Taken together, these results suggest that a combined regimen of Lop plus a PI may be preferentially cytotoxic to colon cancer cells over their normal counterpart cells, thereby providing a safe and effective therapeutic strategy against colon cancer. When we further tested the effect of Btz and/or Lop on other types of cancer cells, we found that Btz/Lop, but not either mono-treatment, very effectively induced the cell death of HeLa (cervical cancer), Caki-1 (renal cancer), T98G (glioma), MDA-MB 435S (breast cancer), and SNU-449 (hepatocellular carcinoma) cells, showing synergy in all five cell lines (Figure 1G and 1H). These results suggest that the potent anticancer effect of Btz/Lop may not be restricted to a particular cancer cell type.

3.2. Neither apoptosis nor autophagy is critically involved in the sensitizing effect of Lop on Btz-mediated cell death in colon cancer cells

To understand how Lop overcomes the resistance of cancer cells to a PI, we performed live-cell imaging in DLD-1 cells treated with Lop and/or Btz. Interestingly, progressive and extensive vacuolation was followed by cell death in DLD-1 cells exposed to Btz/Lop, but not in those exposed to either mono-treatment (Video 1). Btz/Lop treatment initially increased the numbers of small vacuoles; thereafter, the vacuoles increased in size while decreasing in

number. These observations suggest that Btz/Lop induces extensive vacuolation, possibly due to the swelling and fusion of vacuoles, and subsequent cell death. When we examined the cellular morphologies of other colon cancer cells treated with Btz/Lop, we also observed cell death accompanied by vacuolation in SW480, HCT116, and SW-620 cells (Figure 2A). Apoptotic morphologies, including blebbing and apoptotic bodies, were not observed in these cancer cells following treatment with Btz/Lop (Video 1 and Figure 2A). To further assess the possible involvement of apoptosis, we tested the effect of the pan-caspase inhibitor, z-VAD-fmk. However, we found that pretreatment with z-VAD-fmk did not affect the vacuolation or cell death of the Btz/Lop-treated cancer cell lines (Figure 2A and 2B). A flow cytometric assessment of changes in DNA content showed that Lop treatment of DLD-1 cells did not markedly alter the cell cycle profile, whereas Btz treatment induced G_2/M cell cycle arrest (Figure 2C). In DLD-1 cells treated with Btz/Lop for 24 h, the G_1 cell population was decreased compared to that in Lop-treated cultures, but the subG_0/G_1 cell population (5.6%, Figure 2C) was not noticeably increased despite the presence of marked cell death (54.6%, Figure 1A). Furthermore, Btz/Lop treatment did not increase the cleavage of caspase-3 or its substrate, PARP (Figure 2D). Taken together, these results suggest that apoptosis may not be critically involved in the Btz/Lop-induced killing of these cells. We next examined whether Btz/Lop-induced vacuolation and subsequent cell death might be associated with autophagy. We found that while pretreatment of various colon cancer cells with autophagy inhibitors (e.g., 3-MA, BafA, or CQ) had no effect on Btz/Lop-induced vacuolation (Figure 2A), it had a non-significant tendency to increase cell death (Figure 2E). Collectively, these results suggest that an alternative cell death mode may be involved in the anticancer effects induced by Btz/Lop.

3.3. Lop effectively overcomes the resistance of colon cancer cells to Btz by inducing paraptosis-like cell death

Next, we investigated whether Btz/Lop-induced vacuolation is due to changes in organelles, such as the ER and/or mitochondria. To simultaneously observe the ER and mitochondria, we performed confocal microscopy on YFP-ER cells (DLD-1 sublines stably transfected with the YFP-ER plasmid) subjected to MitoTracker-Red (MTR) staining. In YFP-ER cells treated with 20 μM Lop alone, we did not observe any noticeable change in the ER, but the mitochondria notably dilated to a peak at 8 h and then subsequently returned to their original morphology by 24 h. Treatment with 40 nM Btz induced a slight mitochondrial fragmentation from 8 h and generated numerous small ER-derived vacuoles very late at 24 h. In contrast, Btz/Lop induced mitochondrial fragmentation and the progressive fusion-driven expansion of ER-derived vacuoles, which was followed by death-associated cellular detachment (Figure 3A). Except for those occupied by nuclei and fragmented mitochondria, all cellular spaces were occupied with ER-derived vacuoles in YFP-ER cells treated with Btz/Lop for 24 h (Figure 3A). We further observed the ultrastructure of mitochondria and the ER by electron microscopy (EM) and found that treatment of DLD-1 cells with 40 nM Btz alone for 12 h induced mitochondrial fragmentation without any notable change in the ER structure, whereas 20 μM Lop alone induced a fusion-driven increase in the mitochondrial size without any alteration of ER morphology (Figure 3B). In contrast, Btz/Lop treatment for 12 h was associated with the swelling- and fusion-driven generation of ER-derived vacuoles and the presence of fragmented mitochondria. Dilation of the ER and/or mitochondria is a morphological feature of paraptosis [15,16]. Given the above findings and our observation that Lop can transiently induce mitochondrial dilation, we hypothesized that Btz/Lop induces paraptosis-like cell death. Since a common feature of paraptosis is the requirement of *de novo* protein synthesis [15], we tested the effect of the protein synthesis blocker, cycloheximide

(CHX), on the Btz/Lop-induced responses of various colon cancer cells. We found that CHX pretreatment very effectively inhibited the cell death (Figure 3C) and vacuolation (Figure 3D) induced by Btz/Lop in these cells. In addition, CHX pretreatment markedly inhibited the ER dilation, but not the mitochondrial fragmentation, seen in YFP-ER cell treated with Btz/Lop (Figure 3E). Thus, the structural and functional changes of the ER may be more important than those of mitochondria in the anticancer effects of Btz/Lop. Collectively, these results suggest that Btz/Lop kills the tested cancer cells by inducing paraptosis-associated cell death.

3.4. Accumulation of misfolded proteins and CHOP is critical for Btz/Lop-induced paraptosis-like cell death

We next investigated the mechanisms underlying Btz/Lop-induced cancer cell death. Since the main mechanism of cell death induction by PIs involves the accumulation of toxic poly-ubiquitinated proteins and misfolded protein aggregates, which induce ER stress [23], we first examined whether co-treatment with Lop affects these Btz-mediated effects. We found that Lop potentiated the Btz-mediated accumulation of poly-ubiquitinated proteins seen at 8-12 h, but not thereafter (Figure 4A). Immunocytochemical analysis of ubiquitin also showed that Lop co-treatment further increased the Btz-induced accumulation of ubiquitinated proteins to form aggresome-like structures in DLD-1 cells treated with Btz for 12 h (Figure 4B). The Btz/Lop-induced accumulation of poly-ubiquitinated proteins was almost completely blocked by CHX pretreatment (Figure 4B). Additionally, immunostaining of BAP31, a protein abundantly present in the ER membrane [24], revealed that Btz/Lop-induced ER-derived vacuolation was also almost completely blocked by CHX pretreatment (Figure 4B). These results suggest that ongoing protein synthesis may contribute to the accumulation of misfolded proteins within the ER, ER dilation, and eventual cell death. Since proteasome

inhibition was previously shown to induce ER stress and trigger the unfolded protein response (UPR) [25,26], we compared the effects of Btz and/or Lop on these parameters. While the protein levels of PERK and IRE1α were not notably altered in DLD-1 cells treated with Btz and/or Lop, the CHOP upregulation induced by Btz was progressively increased by Lop co-treatment from 8 h. At 16 h, mono-treatment with Btz or Lop increased the CHOP protein level and Btz/Lop co-treatment yielded a more dramatic increase than either mono-treatment (Figure 4C). To investigate the functional significance of CHOP upregulation in Btz/Lop-induced vacuolation and cell death, we examined the effect of siRNA-mediated CHOP knockdown. We found that CHOP knockdown significantly attenuated the cell death (Figure 4D) and vacuolation (Figure 4E) induced by Btz/Lop. To further investigate the involvement of CHOP in Btz/Lop-induced ER vacuolation, we performed immunocytochemical analysis of CHOP and BAP31. We found that siRNA-mediated CHOP knockdown effectively blocked the Btz/Lop-induced nuclear accumulation of CHOP and ER-derived dilation (Figure 4F). Confocal microscopy in YFP-ER cells also showed that CHOP knockdown potently delayed the ability of Btz/Lop to induce ER dilation (Figure 4G). Collectively, these results suggest that CHOP upregulation is critically involved in Btz/Lop-induced ER dilation and subsequent cell death.

3.5. Disruption of Ca^{2+} homeostasis critically contributes to Btz/Lop-induced paraptosis-like cell death

We previously showed that disruption of Ca^{2+} homeostasis plays a crucial role in the paraptosis induced by curcumin [18] or celastrol [20], and other groups showed that Lop can inhibit the L-type Ca^{2+} channel [27] and calmodulin [28]. Therefore, we tested whether Btz/Lop affects intracellular Ca^{2+} levels. Fluorescence microscopy (Figure 5A) and flow

cytometry (Figure 5B) performed using Fluo-3 showed that Btz/Lop progressively and markedly increased cytosolic Ca^{2+} levels, whereas mono-treatment with Btz or Lop triggered only very slight increases in intracellular Ca^{2+} (Figure 5A). When we further measured mitochondrial Ca^{2+} levels using Rhod-2, we found that Btz/Lop progressively increased mitochondrial Ca^{2+} levels, with a peak at 16 h (Figure 5B). To examine the potential significance of a Ca^{2+} imbalance in the cell death induced by Btz/Lop, we investigated the effects of various Ca^{2+} scavengers. Our results revealed that BAPTA, EGTA (scavengers of extracellular Ca^{2+}), and BAPTA-AM (a scavenger of intracellular Ca^{2+}) all had slight but significant inhibitory effects on the cell death induced by Btz/Lop in DLD-1 cells (Figure 5C). Moreover, the co-administration of BAPTA plus BAPTA-AM or EGTA plus BAPTA-AM further inhibited Btz/Lop-induced cell death (Figure 5C). Morphological observation of DLD-1 cells also showed that BAPTA plus BAPTA-AM or EGTA plus BAPTA-AM more notably inhibited Btz/Lop-induced vacuolation and cell death compared to BAPTA, EGTA, or BAPTA-AM alone (Figure 5D). Similar effects on ER-derived vacuolation were observed in YFP-ER cells (Figure 5E). Taken together, these results suggest that an increase in Ca^{2+} (potentially due to an influx of extracellular Ca^{2+}) appears to partially but significantly contribute to the anticancer effects of Btz/Lop. When cytosolic Ca^{2+} levels are high, Ca^{2+} is known to be taken up by mitochondria through the mitochondrial Ca^{2+} uniporter (MCU) [29]. Therefore, to examine whether the increased mitochondrial Ca^{2+} contributes to Btz/Lop-induced cell death, we tested the effect of the MCU inhibitors, ruthenium red or Ru360. We found that pretreatment with ruthenium red or Ru360 did not affect Btz/Lop-induced cell death or vacuolation (Figure 5C and 5D), suggesting that mitochondrial Ca^{2+} overload may not be a direct cause of Btz/Lop-induced paraptosis-like cell death.

3.6. Btz/Lop induces paraptosis-like cell death selectively in colon cancer cells via enhanced ER stress and ER dilation

To investigate the critical signals involved in Btz/Lop-induced paraptosis-like cell death, we first examined the effect of CHX, CHOP knockdown, and Ca^{2+} chelation on the Btz/Lop-induced accumulation of misfolded proteins. We found that while CHX pretreatment almost completely blocked the Btz/Lop-induced accumulation of poly-ubiquitinated proteins, neither CHOP knockdown nor Ca^{2+} chelation (by BAPTA plus BAPTA-AM or EGTA plus BAPTA-AM) had this inhibitory effect (Figure 6A). When we further investigated the effects of these manipulations on the Btz/Lop-induced upregulation of CHOP, we found that Ca^{2+} chelation markedly, but not completely, inhibited the Btz/Lop-induced accumulation of CHOP, whereas CHX pretreatment completely inhibited this effect (Figure 6A). Immunocytochemistry of BAP31 and CHOP revealed that CHX pretreatment almost completely blocked the nuclear accumulation of CHOP, whereas Ca^{2+} chelators remarkably inhibited this parameter (Figure 6B). Our results suggest that the Btz/Lop-induced accumulation of poly-ubiquitinated proteins may lie upstream of the Ca^{2+} increase and CHOP upregulation, and that the Ca^{2+} increase may considerably (if not wholly) mediate the upregulation of CHOP. Fluorescence microscopy performed using Fluo-3 showed that CHX completely blocked the Btz/Lop-induced increase of Ca^{2+}, but CHOP knockdown did not (Figure 6C), again suggesting that the accumulation of misfolded proteins lies upstream of the Ca^{2+} release, and that the increase in Ca^{2+} is not controlled by the upregulation of CHOP. Based on our time-course results and molecular ordering of key signals, we hypothesize that the signaling pathway of Btz/Lop-induced paraptosis-like cell death is as follows: Btz/Lop treatment initially triggers accumulation of misfolded proteins and progressively increases intracellular Ca^{2+} levels, resulting in the induction of CHOP-mediated ER stress, ER dilation and eventually paraptosis-like cell death (Figure 6D).

When we further tested the effect of Btz/Lop on normal colon cells, we found that treatment of CCD-112CoN cells with 40 nM Btz and 20 μM Lop did not induce vacuolation or cell death (Figure 7A), which was notably seen in colon cancer cells exposed to the same treatment (Figure 1A). The Btz/Lop-induced accumulations of poly-ubiquitinated proteins, CHOP (Figure 7B), and Ca^{2+} (Figure 7C) were also much lower in CCD-112CoN cells compared to those in DLD-1 colon cancer cells. These results suggest that Lop may preferentially sensitize colon cancer cells to Btz-mediated cell death by enhancing proteasomal inhibition and Ca^{2+}-mediated ER stress to a greater degree than seen in normal cells. Collectively, our results suggest that the addition of Lop safely and effectively overcomes Btz resistance by inducing paraptosis-like cell death.

4. Discussion

Most of the current anti-cancer therapies trigger apoptosis and related cell death networks to eliminate malignant cells. However, the de-regulation of apoptotic signaling, particularly the activation of an anti-apoptotic system, can allow cancer cells to escape this program, leading to uncontrolled proliferation, tumor survival, therapeutic resistance, and cancer recurrence [30]. In this respect, induction of an alternative cell death mode that uses regulatory mechanisms unlike those of apoptosis and lacks apoptotic features (e.g., apoptotic body formation, chromatin condensation, DNA fragmentation and caspase dependency), could have improved therapeutic effects against cancer cells with innate and acquired apoptotic resistance. An example of such a cell death mode is paraptosis [16]. Therefore, efforts to identify agents or regimens that induce paraptosis or paraptosis-like cell death and/or clarify their underlying mechanisms could support the development of novel therapeutic strategies

for treating resistant malignant cancers. In the present study, we show that Lop, a widely used anti-diarrheal drug, may effectively enhance the anticancer effect of PIs in solid tumors, including colon cancer, by inducing paraptosis-like cell death, while sparing normal colon cells.

Here, we show that while a sublethal dose of Btz failed to induce notable vacuolation or cell death, combination of Btz and Lop at their sublethal concentrations triggered ER-derived vacuolation and cell death. In cells treated with Btz/Lop, mitochondria were fragmented rather than dilated. Similar to our results, Mimnaugh *et al.* [31] reported that the combinations of geldanamycin plus Btz or tunicamycin plus Btz at their sublethal concentrations induced extensive ER-derived vacuolization. They proposed that this ER vacuolization was due to a massive buildup of misfolded proteins within the ER lumen; this would exert an osmotic force that would induce an influx of water from the cytoplasm and distend the ER into vacuoles. We presume that extensive fusion among the swollen ER membranes could critically contribute to irreversibly impairing the structure and function of the ER, thereby leading to cancer cell death.

Analysis of the Btz/Lop-induced ER stress responses revealed that Lop cotreatment initially accelerated the Btz-mediated accumulation of poly-ubiquitinated proteins, and that this was very effectively blocked by CHX pretreatment. In addition to triggering ER-derived vacuolation, Btz/Lop progressively increased cytosolic Ca^{2+} levels. Treatment with BAPTA (or EGTA) plus BAPTA-AM significantly, but not completely, inhibited Btz/Lop-induced vacuolation and cell death. As ER stress is known to trigger the UPR to restore ER homeostasis [32], we tested the possible involvement of various UPR components, including IRE1α, PERK, and CHOP. We found that Lop cotreatment most dramatically enhanced the Btz-induced nuclear expression of CHOP. Moreover, CHOP knockdown effectively inhibited

Btz/Lop-mediated paraptosis-like cell death, suggesting that this protein plays a critical role in the process. Finally, we examined the correlations among the accumulation of misfolded proteins, the increase in Ca^{2+}, and the upregulation of CHOP, in Btz/Lop-induced paraptosis-like cell death. Time-course assessment of key signals and detailed analyses employing CHX, Ca^{2+} chelators, and CHOP siRNA revealed that Lop aggravates Btz-mediated ER stress and ER vacuolation by enhanced accumulation of misfolded proteins and by perturbing Ca^{2+} homeostasis. Additionally, we found that both accumulation of misfolded proteins and increased Ca^{2+} levels critically contribute to Btz/Lop-induced CHOP upregulation. Studies have shown that CHOP acts as a specific and convergent transcription factor for ER stress [33]. In addition, CHOP also indirectly regulates apoptosis by controlling the expression of pro-apoptotic or anti-apoptotic genes, including those involved in the Bcl-2-mediated intrinsic and DR5-mediated extrinsic apoptotic pathways [34,35]. However, although ongoing research supports the existence of CHOP-mediated apoptotic signaling networks, other studies have suggested that CHOP may also have non-apoptotic involvements in developing pathologies [36]. We recently reported that CHOP contributes to ER-derived vacuolation and subsequent cell death in curcumin- or dimethoxycurcumin-induced paraptosis [19] and in ophiobolin A-induced paraptosis-like cell death [37]. Taken together, these results suggest that CHOP upregulation may be a key mediator of ER-derived vacuolation in paraptosis and paraptosis-like cell death. Future work is needed to clarify the downstream targets of CHOP that are directly involved in ER-derived vacuolation during paraptosis. Recent studies have shown that clarithromycin (a semi-synthetic antibiotic) [38], nelfinavir (an HIV protease inhibitor) [39], and nutlin-3 [21] effectively enhance Btz-mediated cytotoxicity, and that CHOP upregulation plays a crucial and common role in such effects. These results suggest that designing a combination regimen to potently enhance CHOP upregulation could critically improve PI-based cancer therapy.

It is intriguing to consider the underlying mechanism through which Ca^{2+} levels are increased during Btz/Lop-induced paraptosis-like cell death. We note that Lop blocks L-type calcium channels at submicromolar concentrations and blocks high voltage-dependent calcium channels at high micromolar concentrations [27]. In addition, proteasome inhibition blocks the degradation of the major ER Ca^{2+} release channel, IP_3Rs [40]. Therefore, additional work is needed to clarify how Btz and Lop cooperatively increase the influx of extracellular Ca^{2+} and the level of cytosolic Ca^{2}. Furthermore, it remains to be elucidated whether impaired Ca^{2+} homeostasis is directly associated with the enhanced accumulation of misfolded proteins seen during Btz/Lop-induced paraptosis-like cell death.

Studies have shown that Lop displays cytotoxicity and apoptosis-inducing activity in several human tumor cell lines [41], triggers autophagy-dependent cell death in glioblastoma cells [42] and reverses multidrug resistance in a doxorubicin-resistant breast cancer cell line [43]. The latter two findings suggested that Lop could prove useful as a sensitizer of chemotherapy. In the present study, we show for the first time that sublethal doses of Lop effectively can overcome the resistance of colon cancer cells to PIs by inducing paraptosis-like cell death. Diarrhea is a common side effect observed in MM or mantle cell lymphoma patients treated with Btz (diarrhea occurs in 51% of patients, with 8% of the events being severe) [44] and Lop is commonly recommended as a treatment for chemotherapy-related diarrhea in cancer patients [45]. Therefore, a combined regimen of PI plus Lop may have many advantages, such as lower toxicity due to the ability to reduce the PI dose, more widespread applicability to solid tumors, and lower therapeutic cost because it combines a reduced dose of PI, which is expensive, with Lop, which is inexpensive (one percent price of paclitaxel). Furthermore, it should be relatively easy to perform clinical trials using Lop and PIs, since their safety profiles, pharmacokinetics, and metabolism have already been established [46]. The clinical application of Lop in PI-based cancer therapy may therefore significantly benefit cancer

patients in its effectiveness, safety, and therapeutic cost, while potentially expanding the applicability of PIs to solid tumors. This is the first study showing the potential sensitizing effect of Lop on PI-mediated cell death. The significance of our results should be confirmed by *in vivo* experiments using xenograft models. In addition, to support the successful clinical translation of our findings, further experiments will be needed to optimize various aspects of the combined regimen, including the dosing, formulations and administration routes of Lop and Btz, are warranted.

Conflict of interest

The authors declare that they have no competing interests.

Acknowledgements

This work was supported by grants from the Korean Health Technology R&D Project, Ministry of Health & Welfare (HI18C0263) and NRF-2018R1D1A1B07047560.

References

[1] U. Schubert, L.C. Antón, J. Gibbs, C.C. Norbury, J.W. Yewdell, J.R. Bennink, Rapid degradation of a large fraction of newly synthesized proteins by proteasomes, Nature 404 (6779) (2000) 770-774, http://doi.org/10.1038/35008096.

[2] E. E. Manasanch, R. Z. Orlowski, Proteasome inhibitors in cancer therapy, Nat. Rev. Clin. Oncol. 14 (7) (2017) 417-433, http://doi.org/10.1038/nrclinonc.2016.206.

[3] R. Z. Orlowski, E. C. Dees, The role of the ubiquitination-proteasome pathway in breast cancer: applying drugs that affect the ubiquitin-proteasome pathway to the therapy of breast cancer. Breast Cancer Res. 5 (1) (2003) 1-7, http://doi.org/10.1186/bcr460.

[4] S. Frankland-Searby, S.R. Bhaumik, The 26S proteasome complex: an attractive target for cancer therapy, Biochim. Biophys. Acta. 1825 (1) (2012) 64-76, http://doi.org/10.1016/j.bbcan.2011.10.003.

[5] S. Gandolfi, J.P. Laubach, T. Hideshima, D. Chauhan, K.C. Anderson, P.G. Richardson, The proteasome and proteasome inhibitors in multiple myeloma, Cancer Metastasis Rev. 36 (4) (2017) 561-584, http://doi.org/10.1007/s10555-017-9707-8.

[6] A. Field-Smit, G.J. Morgan, F.E. Davies, Bortezomib (velcadetrade mark) in the treatment of multiple myeloma. Ther. Clin. Risk Manag. 2(3) (2006) 271-279.

[7] M.S.F. Roeten, J. Cloos, G. Jansen, Positioning of proteasome inhibitors in therapy of solid malignancies, Cancer Chemother. Pharmacol. 81 (2) (2018) 227-243, http://doi.org/10.1007/s00280-017-3489-0.

[8] B. Faiman, Diarrhea in multiple myeloma: a review of the literature, Clin. J. Oncol. Nurs. 20 (4) (2016) E100-105, http://doi.org/10.1188/16.CJON.E100-E105.

[9] J.J. Driscoll, A. Minter, D.A. Driscoll, J.K. Burris, The ubiquitin+proteasome protein degradation pathway as a therapeutic strategy in the treatment of solid tumor malignancies, Anticancer Agents Med. Chem. 11 (2) (2011) 242-246.

[10] Z. Huang, Y. Wy, X. Zhou, J. Xu, W. Zhu, Y. Shu, P. Liu, Efficacy of therapy with

bortezomib in solid tumors: a review based on 32 clinical trials, Future Oncol. 10 (10) (2014) 1795-1807, http://doi.org/10.2217/fon.14.30.

[11] K.P. Papadopoulos, H.A.3rd Burris, M. Gordon, P. Lee, E.A. Sausville, P.J. Rosen, R.E. Jr. Cutler, Z. Wang, S. Lee, S.F. Jones, J.R. Infante, A phase I/II study of carfilzomib 2-10-min infusion in patients with advanced solid tumors, Cancer Chemother. Pharmacol. 72 (4) (2013) 861-868, http://doi.org/10.1007/s00280-013-2267-x.

[12] R.A. Kyle, S.V. Rajkumar, Treatment of multiple myeloma: a comprehensive review, Clin. Lymphoma Myeloma 9 (4) (2009) 278-288, http://doi.org/10.3816/CLM.2009.n.056.

[13] L. Menéndez, A. Lastra, A. Meana, A. Hidalgo, A. Baamonde, Analgesic effect of loperamide in bone cancer pain in mice, Pharmacol. Biochem. Behav. 81 (1) (2005) 114-121, http://doi.org/10.1016/j.pbb.2005.02.007.

[14] R. Kumar, Loperamide: from antidiarrheal to analgesic, J. Opioid Manag. 9 (4) (2013) 301-302, http://doi.org/10.5055/jom.2013.0172.

[15] S. Sperandio, I. de Belle, D.E. Bredesen, An alternative, nonapoptotic form of programmed cell death, Proc. Natl. Acad. Sci. USA. 97 (26) (2000) 14376-14381, http://doi.org/10.1073/pnas.97.26.14376.

[16] D. Lee, I.Y. Kim, S. Saha, K.S. Choi, Paraptosis in the anti-cancer arsenal of natural products, Pharmacol. Ther. 162 (2016) 120-133, http://doi.org/10.1016/j.pharmthera.2016.01.003.

[17] M.J. Yoon, E.H. Kim, J.H. Lim, T.K. Kwon, K.S. Choi, Superoxide anion and proteasomal dysfunction contribute to curcumin-induced paraptosis of malignant breast cancer cells, Free Radic. Biol. Med. 48 (5) (2010) 713-726, http://doi.org/10.1016/j.freeradbiomed.

[18] M.J. Yoon, E.H. Kim, T.K. Kwon, S.A. Park, K.S. Choi, Simultaneous mitochondrial Ca(2+)overload and proteasomal inhibition are responsible for the induction of paraptosis in

malignant breast cancer cells, Cancer Lett. 324 (2) (2012) 197-209, http://doi.org/10.1016/j.canlet.2012.05.018.

[19] M.J. Yoon, Y.J Kang, J.A. Lee, I.Y. Kim, M.A. Kim, Y.S. Lee, J.H. Park, B.Y. Lee, I.A. Kim, H.S. Kim, S.A. Kim, A.R. Yoon, C.O. Yun, E.Y. Kim, K. Lee, K.S. Choi, Stronger proteasomal inhibition and higher CHOP induction are responsible for more effective induction of paraptosis by dimethoxycurcumin than curcumin, Cell Death Dis. 5 (2014) e1112, http://doi.org/10.1038/cddis.2014.85.

[20] M.J. Yoon, A.R. Lee, S.A. Jeong, Y.S. Kim, J.Y. Kim, Y.J. Kwon, K.S. Choi, Release of Ca2+ from the endoplasmic reticulum and its subsequent influx into mitochondria trigger celastrol-induced paraptosis in cancer cells, Oncotarget 5 (16) (2014) 6816-6831, http://doi.org/10.18632/oncotarget.2256.

[21] D.M. Lee, I.Y. Kim, M.J. Seo, M.R. Kwon, K.S. Choi, Nutlin-3 enhances the bortezomib sensitivity of p53-defective cancer cells by inducing paraptosis, Exp. Mol. Med. 49 (8) (2017) e365, http://doi.org/10.1038/emm.2017.112.

[22] T.C. Chou, P. Talalay, Quantitative analysis of dose-effect relationship: the combined effects of multiple drugs or enzyme inhibitors, Adv. Enzyme Regul. 22 (1984) 27-55.

[23] W.X. Ding, H.M. Ni, W. Gao, T. Yoshimori, D.B. Stolz, D. Ron, X.N. Yin, Linking autophagy to ubiquitin-proteasome system is important for the regulation of endoplasmic reticulum stress and cell viability, Am. J. Pathol. 171 (2) (2017) 513-524, http://doi.org/10.2353/ajpath.2007.070188.

[24] W.G. Annaert, B. Becker, U. Kistner, M. Reth, R. Jahn, Export of cellubrevin from the endoplasmic reticulum is controlled by BAP31, J. Cell Biol. 139 (6) (1997) 1397-1410.

[25] A.H. Lee, N.N. Iwakoshi, K.C. Anderson, L.H, Glimcher, Proteasome inhibitors disrupt

the unfolded protein response in myeloma cells, Proc. Natl. Acad. Sci. USA. 100 (17) (2003) 9946-9951, http://doi.org/10.1073/pnas.1334037100.

[26] S.T. Nawrocki, J.S. Carew, K.Jr. Dunner, L.H. Boise, P.J. Huang, J.L Abbruzzese, D.J. McConkey, Bortezomib inhibits PKR-like endoplasmic reticulum (ER) kinase and induces apoptosis via ER stress in human pancreatic cancer cells, Cancer Res. 65 (24) (2005) 11510-11519, http://doi.org/10.1158/0008-5472.

[27] J. Church, E.J. Fletcher, K. Abdel-Hamid, J.F. MacDonald, Loperamide blocks high-voltage-activated calcium channels and N-methyl-D-aspartate-evoked responses in rat and mouse cultured hippocampal pyramidal neurons, Mol. Pharmacol. 45 (4) (1994) 747-757.

[28] J.H. Zavecz, T.E. Jackson, G.L. Limp, T.O. Yellin, Relationship between anti-diarrheal activity and binding to calmodulin, Eur. J. Pharmacol. 78 (3) (1982) 375-377.

[29] D. de Stefani, M. Patron, R. Rizzuto, Structure and function of the mitochondrial calcium uniporter complex, Biochim. Biophys. Acta 1853 (9) (2015) 2006-2011, http://doi.org/10.1016/j.bbamcr.2015.04.008.

[30] R.M Mohammad, I. Mugbil, L. Lowe, C. Yedjou, H.Y. Hsu, L.T. Lin, M.D. Siegelin, C. Fimognari, N.B. Kumar, Q.P. Dou, H. Yang, A.K. Samadi, G.L. Russo, C. Spagnuolo, S.K. Ray, M. Chakrabarti, J.D. Morre, H.M. Coley, K. Honoki, H, Fujii, A.G. Georgakilas, A. Amedei, E. Niccolai, A. Amin, S.S. Ashraf, W.G. Helferich, X. Yang, C.S. Boosani, G. Guha, D. Bhakta, M.R. Ciriolo, K. Aquilano, S. Chen, S.I. Mohammed, W.N. Keith, a. Bilsland, D. Halicka, S. Nowsheen, A.S. Azmi, Broad targeting of resistance to apoptosis in cancer, Semin. Cancer Biol. 35 (2015) S78-S103, http://doi.org/10.1016/j.semcancer. 2015.03.001.

[31] E.G. Mimnaugh, W. Xu, M. Vos, X. Yuan, L. Neckers, Endoplasmic reticulum vacuolization and valosin-containing protein relocalization result from simultaneous Hsp90 inhibition by geldanamycin and proteasome inhibition by velcade, Mol. Cancer Res. 4 (9)

(2006) 667-681, http://doi.org/10.1158/1541-7786.MCR-06-0019.

[32] L. Zhao, S.L. Ackeman, Endoplasmic reticulum stress in health and disease, Curr. Opin. Cell Biol. 18 (4) (2006) 444-452, http://doi.org/10.1016/j.ceb.2006.06.005.

[33] R. Kim, T. Toge, Changes in therapy for solid tumors: potential for overcoming drug resistance in vivo with molecular targeting agents, Surg. Today 34 (4) (2004) 293-303, http://doi.org/10.1007/s00595-003-2710-4.

[34] S. Oyadomari, M. Mori, Role of CHOP/GADD153 in endoplasmic reticulum stress, Cell Death Differ. 11 (4) (2004) 381-389, http://doi.org/10.1038/sj.cdd.4401373

[35] R. Sano, J.C. Reed, ER stress-induced cell death mechanisms, Biochim. Biophys. Acta 1833 (12) (2013) 3460-3470, http://doi.org/10.1016/j.bbamcr.2013.06.028

[36] Y. Yang, L. Liu, I. Naik, Z. Braunstein, J. Zhong, B. Ren, Transcription Factor C/EBP Homologous Protein in Health and Diseases, Front Immunol. 8 (2017) 1612, http://doi.org/10.3389/fimmu.2017.01612.

[37] I.Y. Kim, M. Kwon, M.K. Choi, D. Lee, D.M. Lee, M.J. Seo, K.S. Choi, Ophiobolin A kills human glioblastoma cells by inducing endoplasmic reticulum stress via disruption of thiol proteostasis, Oncotarget 8 (63) (2017) 106740-106752, http://doi.org/10.18632/oncotarget.22537.

[38] S. Komatsu, K. Miyazawa, S. Moriya, A. Takase, M. Naito, M. Inazu, N. Kohno, M. Itoh, A. Tomoda, Clarithromycin enhances bortezomib-induced cytotoxicity via endoplasmic reticulum stress-mediated CHOP (GADD153) induction and autophagy in breast cancer cells, Int. J. Oncol. 40 (2012) 1029-1039, http://doi.org/10.3892/ijo.2011.1317.

[39] S. Kawabata, J.J. Gills, J.R. Mercado-Matos, J. Lopiccolo, W. 3rd Wilson, M.C. Hollander, P.A. Dennis, Synergistic effects of nelfinavir and bortezomib on proteotoxic death of NSCLC and multiple myeloma cells, Cell Death Dis. 3 (2012) e353, http://doi.org/10.1038/cddis.2012.87.

[40] D.A. Sliter, K. Kubota, D.S. Kirkpatrick, K.J. Alzayady, S.P. Gygi, R.J. Wojcikiewicz, Mass spectrometric analysis of type 1 inositol 1,4,5-trisphosphate receptor ubiquitination, J. Biol. Chem. 283 (51) (2008) 35319-35328, http://doi.org/10.1074/jbc.M807288200

[41] X.W. Gong, Y.H. Xu, X.L. Chen, Y.X. Wang, Loperamide, an antidiarrhea drug, has antitumor activity by inducing cell apoptosis, Pharmacol. Res. 65 (3) (2012) 372-378, http://doi.org/10.1016/j.phrs.2011.11.007.

[42] S. Zielke, N. Meyer, M. Mari, K. Abou-El-Ardat, F. Reggiori, S.J.L. van Wijk, D. Kögel, S. Fulda, Loperamide, pimozide, and STF-62247 trigger autophagy-dependent cell death in glioblastoma cells, Cell Death Dis. 9 (10) (2018) 994, http://doi.org/10.1038/s41419-018-1003-1.

[43] Y. Zhou, R. Sridhar, L. Shan, W. Sha, X. Gu, S. Sukumar, Loperamide, an FDA-approved antidiarrhea drug, effectively reverses the resistance of multidrug resistant MCF-7/MDR1 human breast cancer cells to doxorubicin-induced cytotoxicity, Cancer Invest. 30 (2) (2012) 119-125, http://doi.org/10.3109/07357907.2011.640653.

[44] J.R. Berenson, S. Jagannath, B. Barlogie, D.T. Siegel, R. Alexanian, P.G. Richardson, D. Irwin, M. Alsina, S.V. Rajkumar, G. Srkalovic, S. Singhal, S. Limentani, R. Niesvizky, D.L. Esseltine, E. Trehu, D.P. Schenkein, K. Anderson, Safety of prolonged therapy with bortezomib in relapsed or refractory multiple myeloma, Cancer 104 (4) (2005) 2141-2148, http://doi.org/10.1002/cncr.21427.

[45] A. Stein, W. Voigt, K. Jordan, Chemotherapy-induced diarrhea: pathophysiology, frequency and guideline-based management, Ther. Adv. Med. Oncol. 2 (1) (2010) 51-63, http://doi.org/10.1177/1758834009355164.

[46] D.E. Baker, Loperamide: a pharmacological review, Rev. Gastroenterol. Disord. 7 (2007) S11-S18.

Figure Legends

Figure 1. Lop sensitizes various colon cancer cells, but not normal colon cells, to PI-mediated cell death.

(A, D, F, G) Cells were treated with the indicated concentrations of PIs and/or Lop for 24 h and cellular viability was assessed using the IncuCyte system, as described in the Materials and Methods. The percentage of live cells was normalized to that of untreated control cells (100%). Data represent the mean ± SD. One-way ANOVA and Bonferroni's post hoc test. *P<0.005, **P<0.01 vs. PI treated cells. (B, E, H) Isoboles for the combinations of PIs and Lop that proved isoeffective (IC_{50}) for inhibiting cell viability. (C) DLD-1 cells were treated with 40 nM Btz and/or 20 μM Lop for 4 h, and clonogenic assays were performed as described in the Materials and Methods. Colony-forming units were enumerated and are expressed as the percentages of control cells. Representative dishes are shown for the clonogenic assay.

Figure 2. Combined treatment with Btz and Lop induces non-apoptotic and non-autophagic cell death.

(A) Cells were treated with Btz and/or Lop (for DLD-1 and SW-480 cells, 40 nM Btz and/or 20 μM Lop; for HCT116 and SW-620 cells, 5 nM Btz and/or 20 μM Lop) for 24 h. To test the involvement of apoptosis or autophagy in the vacuolation and cell death induced by Btz/Lop, cells were pretreated with 20 μM z-VAD-fmk (an apoptosis inhibitor), 400 μM 3-MA, 20 nM BafA, or 20 μM CQ (autophagy inhibitors) and further treated with Btz/Lop for 24 h. Cellular morphologies were observed by phase-contrast microscopy. Bars, 40 μm. (B, E) Cells were pretreated with the indicated inhibitor and further treated with the indicated concentrations of Btz/Lop for 24 h. Cellular viability was assessed using the IncuCyte system.

Data represent the mean ± SD. One-way ANOVA and Bonferroni's post hoc test. *P<0.005 vs. untreated cells. (C) DLD-1 cells were treated with 40 nM Btz and/or 20 μM Lop for 24 h. Flow cytometry was performed to measure DNA content. (D) DLD-1 cells were treated with 40 nM Btz and/or 20 μM Lop for the indicated time durations. Western blotting of the indicated proteins was performed, with α-tubulin used as a loading control *(left)*. The relative intensities of p43 caspase-3 and PARP were obtained by densitometry using the ImageJ software and are presented relative to the level of α-tubulin (*right*).

Figure 3. Lop effectively overcomes Btz resistance by inducing paraptosis-like cell death.

(A) YFP-ER cells were treated with 40 nms. Btz and/or 20 μM Lop for the indicated time durations and then stained with MitoTracker-Red (MTR). Cells were observed by confocal microscopy. Bars, 30 μm. (B) Transmission electron microscopy of DLD-1 cells treated with 40 nM Btz and/or 20 μM Lop for 12 h. Bars, 500 nm. (C) Cells were pretreated with CHX for 30 min and then treated with the indicated concentrations of Btz and/or Lop for 24 h, and cellular viability was assessed using the IncuCyte system. Data represent the mean ± SD. One-way ANOVA and Bonferroni's post hoc test. *P<0.005 vs. untreated cells; #P<0.005 vs. cells treated with Btz/Lop. (D) Cells were pretreated with 2 μM CHX for 30 min, treated with Btz/Lop at the concentrations indicated in (C) for 24 h, and observed by phase-contrast microscopy. Bars, 40 μm. (E) YFP-ER cells were pretreated with CHX for 30 min, treated with 40 nM Btz and/or 20 μM Lop for the indicated time durations, stained with MTR, and observed under the confocal microscope. Bars, 30 μm.

Figure 4. Accumulation of misfolded proteins and CHOP is critically involved in Btz/Lop-induced paraptosis-like cell death.

(A, C) DLD-1 cells were treated with 40 nM Btz and/or 20 μM Lop for the indicated time

durations. Western blotting of the indicated proteins was performed, with α-tubulin used as a loading control. LE and SE denote long exposure and short exposure, respectively (C *upper*). The relative intensities of IRE1, PERK and CHOP (LE) were obtained by densitometry and are presented relative to the level of α-tubulin (C *lower*). One-way ANOVA and Bonferroni's post hoc test. *P<0.001 vs. untreated cells; #P<0.001 vs. Btz-treated cells. (B) DLD-1 cells were treated with 40 nM Btz and/or 20 μM Lop for 12 h. Immunocytochemistry of Ub and BAP31 and DAPI counterstaining of nuclei were performed. To investigate the effect of CHX, DLD-1 cells were pretreated with 2 μM CHX and further treated with Btz and Lop for 12 h. Bar, 30 μm. (D-F) DLD-1 cells were transfected with the negative control siRNA (siNC) or a CHOP-targeting siRNA (siCHOP) for 24 h and further treated with the indicated concentrations of Btz/Lop for 24 h or for the indicated time durations, if specified. (D) Cellular viability was assessed using the IncuCyte system (*upper*). Data represent the mean ± SD. One-way ANOVA and Bonferroni's post hoc test. *P<0.005 vs. cells transfected with siNC and further treated with Btz/Lop. Knockdown of CHOP was confirmed by Western blotting, with α-tubulin used as a loading control. The relative intensities of CHOP were obtained by densitometry and are presented relative to the level of α-tubulin (*lower*). One-way ANOVA and Bonferroni's post hoc test. *P<0.001 vs. untreated cells transfected with siNC. (E) Cellular morphologies were observed by phase-contrast microscopy. Bars, 40 μm. (F) Immunocytochemistry of BAP31 and CHOP and DAPI counterstaining of nuclei were performed. Bars, 30 μm. (G) YFP-ER cells were transfected with siNC or siCHOP for 24 h, treated with 40 nM Btz plus 20 μM Lop for the indicated time durations, and observed under the confocal microscope. Bars, 30 μm.

Figure 5. Increase in intracellular Ca^{2+} critically contributes to Btz/Lop-induced

paraptosis-like cell death.

(A, B) DLD-1 cells were treated with 40 nM Btz and/or 20 μM Lop for the indicated time durations. (A) Btz/Lop-treated cells were stained with Fluo-3 and subjected to fluorescence microscopy. Bars, 40 μm. (B) Btz/Lop-treated cells were stained with Fluo-3 or Rhod-2 and subjected to flow cytometry. (C) DLD-1 cells were pretreated with the indicated calcium antagonist(s) for 30 min, and further treated with 40 nM Btz plus 20 μM Lop for 24 h. Cellular viability was assessed using the IncuCyte system, as described in the Materials and Methods. Data represent the means ± SD. One-way ANOVA and Bonferroni's post hoc test. *P<0.005 vs. untreated cells; #P<0.005 vs. cells treated with Btz/Lop. (D) DLD-1 cells were pretreated with 10 μM BAPTA, 0.5 mM EGTA, 10 μM BAPTA-AM, 10 μM BAPTA plus 10 μM BAPTA-AM, 0.5 mM EGTA plus 10 μM BAPTA-AM, 5 μM ruthenium red, or 20 μM Ru360 for 30 min, and further treated with 40 nM Btz plus 20 μM Lop for 24 h. Cellular morphologies were observed by phase-contrast microscopy. Bars, 40 μm. (E) YFP-ER cells were pretreated with the indicated calcium chelators for 30 min, treated with 40 nM Btz plus 20 μM Lop for the indicated time durations and observed under the confocal microscope. Bars, 30 μm.

Figure 6. Molecular ordering of key signals involved in Btz/Lop-induced paraptosis-like cell death.

(A) DLD-1 cells were pretreated with 2 μM CHX, transfected with siNC or siCHOP, or pretreated with the indicated Ca^{2+} chelators, and then treated with 40 nM Btz and 20 μM Lop for 16 h. Cell extracts were subjected to Western blotting of the indicated proteins, with α-tubulin used as a loading control (*upper*). The relative intensities of CHOP were obtained by densitometry and are presented relative to the level of α-tubulin (*lower*). One-way ANOVA and Bonferroni's post hoc test. *P<0.001 vs. untreated cells; #P<0.001 vs. cells exposed to

Btz/Lop with no further treatment. (B) DLD-1 cells were pretreated with 2 μM CHX, 10 μM BAPTA plus 10 μM BAPTA-AM, or 0.5 mM EGTA plus 10 μM BAPTA-AM for 30 min, and further treated with Btz/Lop for 16 h. Immunocytochemistry of BAP31 and CHOP and DAPI counterstaining of nuclei were performed. Bars, 30 μm. (C) DLD-1 cells were pretreated with CHX or transfected with siNC or siCHOP and then further treated with Btz/Lop for 16h. Cells were stained with Fluo-3 and observed by fluorescence and phase-contrast microscopy. Bars, 40 μm. (D) Hypothetical model of the signaling pathways involved in Btz/Lop-induced paraptosis-like cell death.

Figure 7. Paraptosis-like cell death accompanied by ER stress and ER dilation is not induced in normal colon cells treated with Btz/Lop.

(A) Morphologies of CCD-112CoN cells treated with 40 nM Btz and/or 20 μM Lop for 24 h, as observed by phase-contrast microscopy. Bars, 40 μm. (B, C) CCD-112CoN and DLD-1 cells were treated with 40 nM Btz plus 20 μM Lop for 24 h. (B) Cell extracts were subjected to Western blotting of the indicated proteins, with α-tubulin used as a loading control (*left*). The relative intensities of CHOP were obtained by densitometry and are presented relative to the level of α-tubulin (*right*). One-way ANOVA and Bonferroni's post hoc test. *P<0.001 vs. CCD-112 CoN cells exposed to Btz/Lop. (C) Treated cells were stained with Fluo-3 and subjected to fluorescence microscopy. Bars, 40 μm.

Video 1. Live-cell imaging of DLD-1 cells treated with Btz and/or Lop.

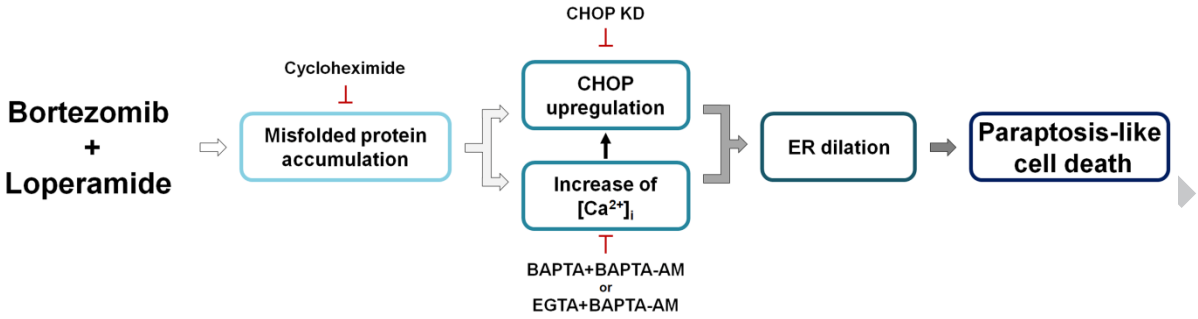

Figure 1. Lop sensitizes various colon cancer cells, but not normal colon cells, to PI-mediated cell death.

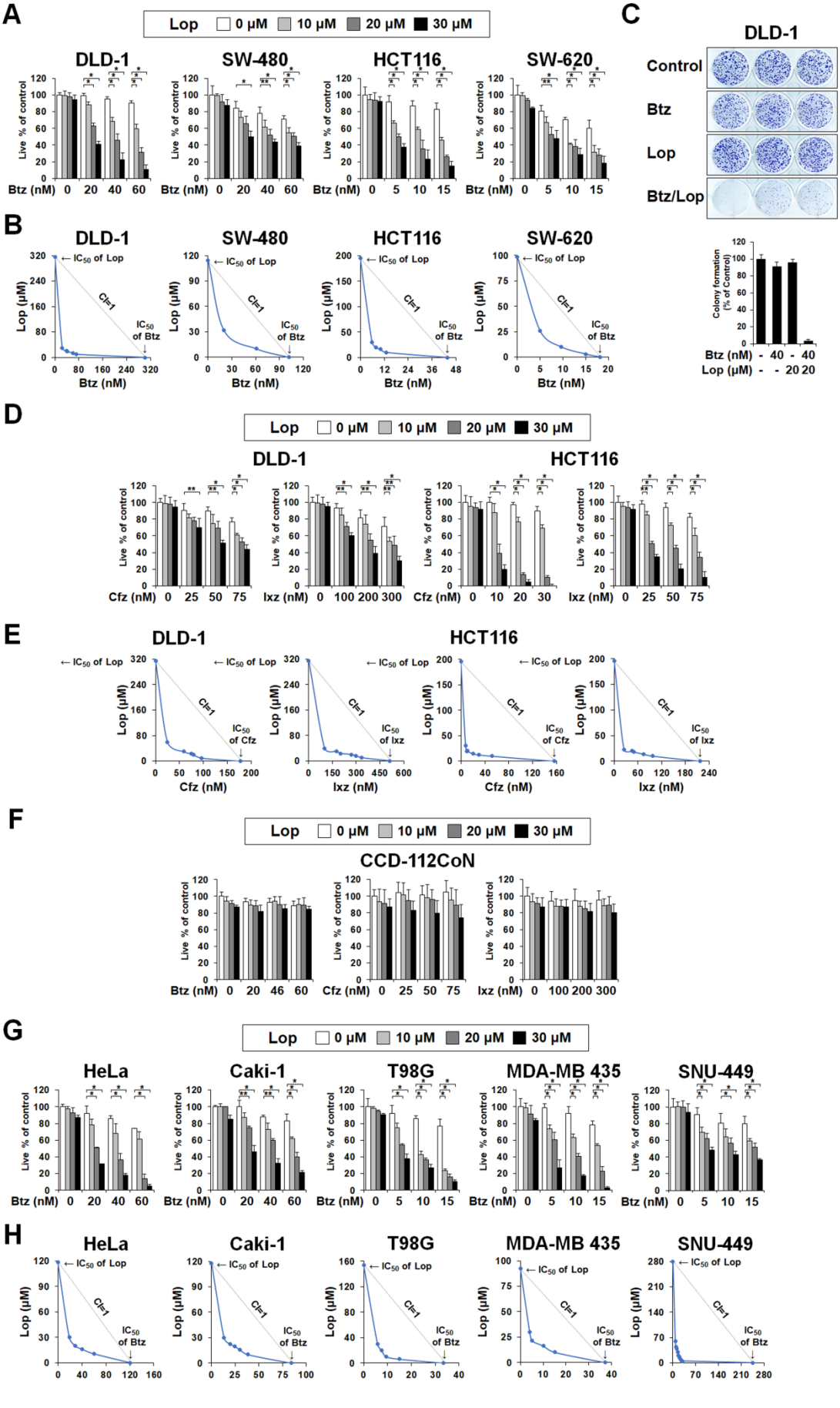

Figure 2. Combined treatment with Btz and Lop induces non-apoptotic and non-autophagic cell death.

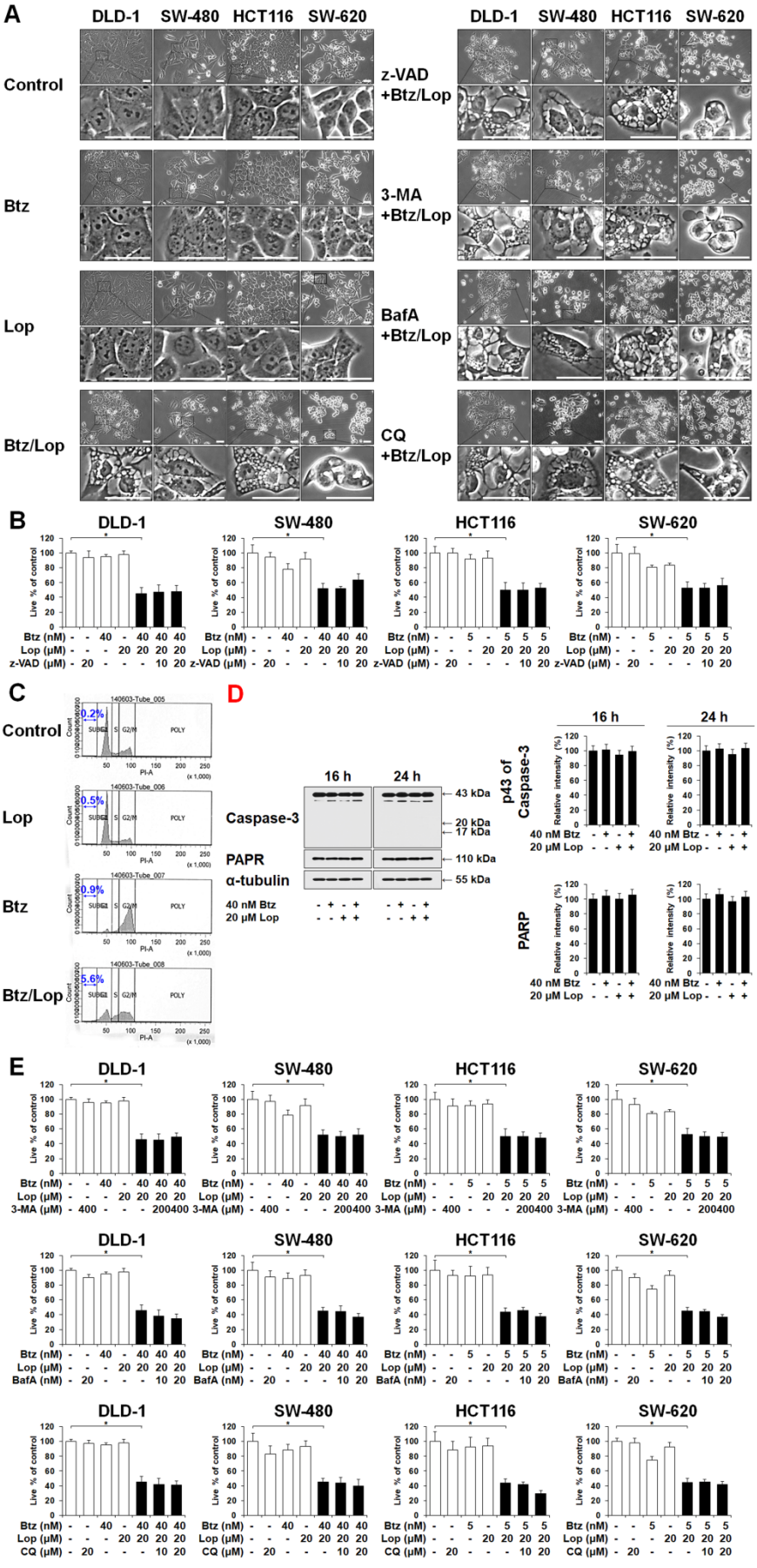

Figure 3. Lop effectively overcomes Btz resistance by inducing paraptosis-like cell death.

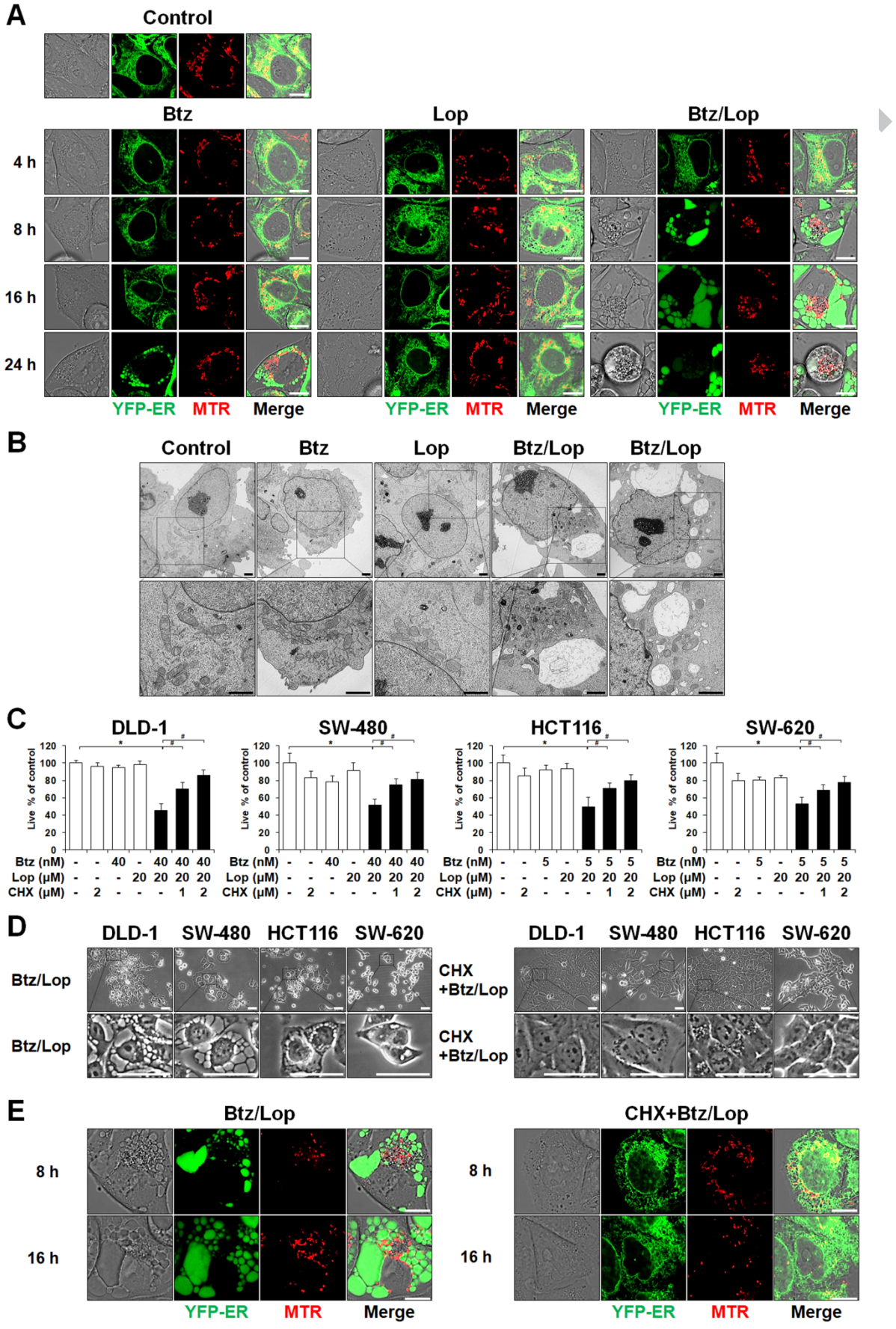

Figure 4. Accumulation of misfolded proteins and CHOP is critically involved in Btz/Lop induced paraptosis-like cell death.

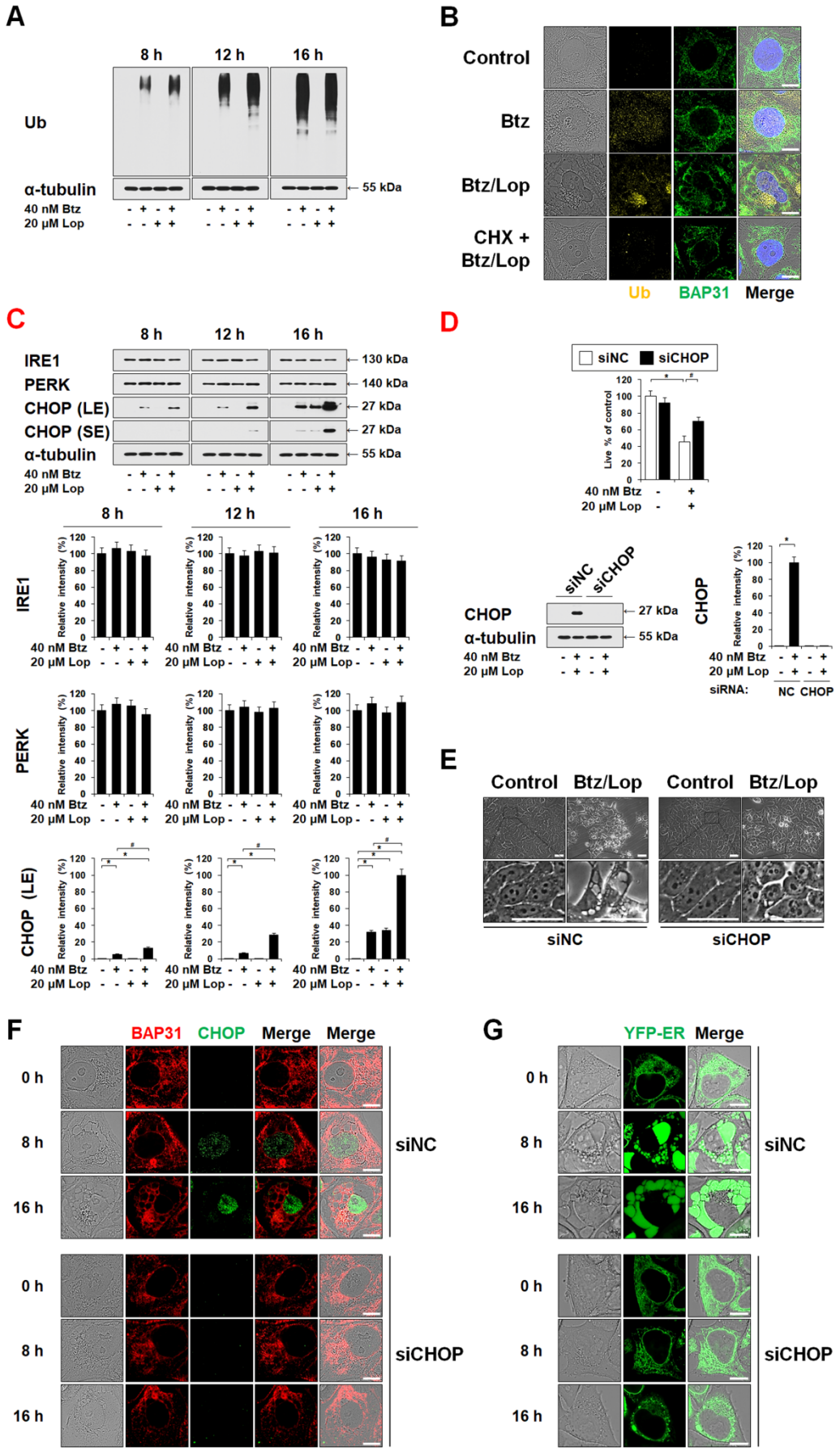

Figure 5. Increase in intracellular Ca^{2+} critically contributes to Btz/Lop-induced paraptosis-like cell death.

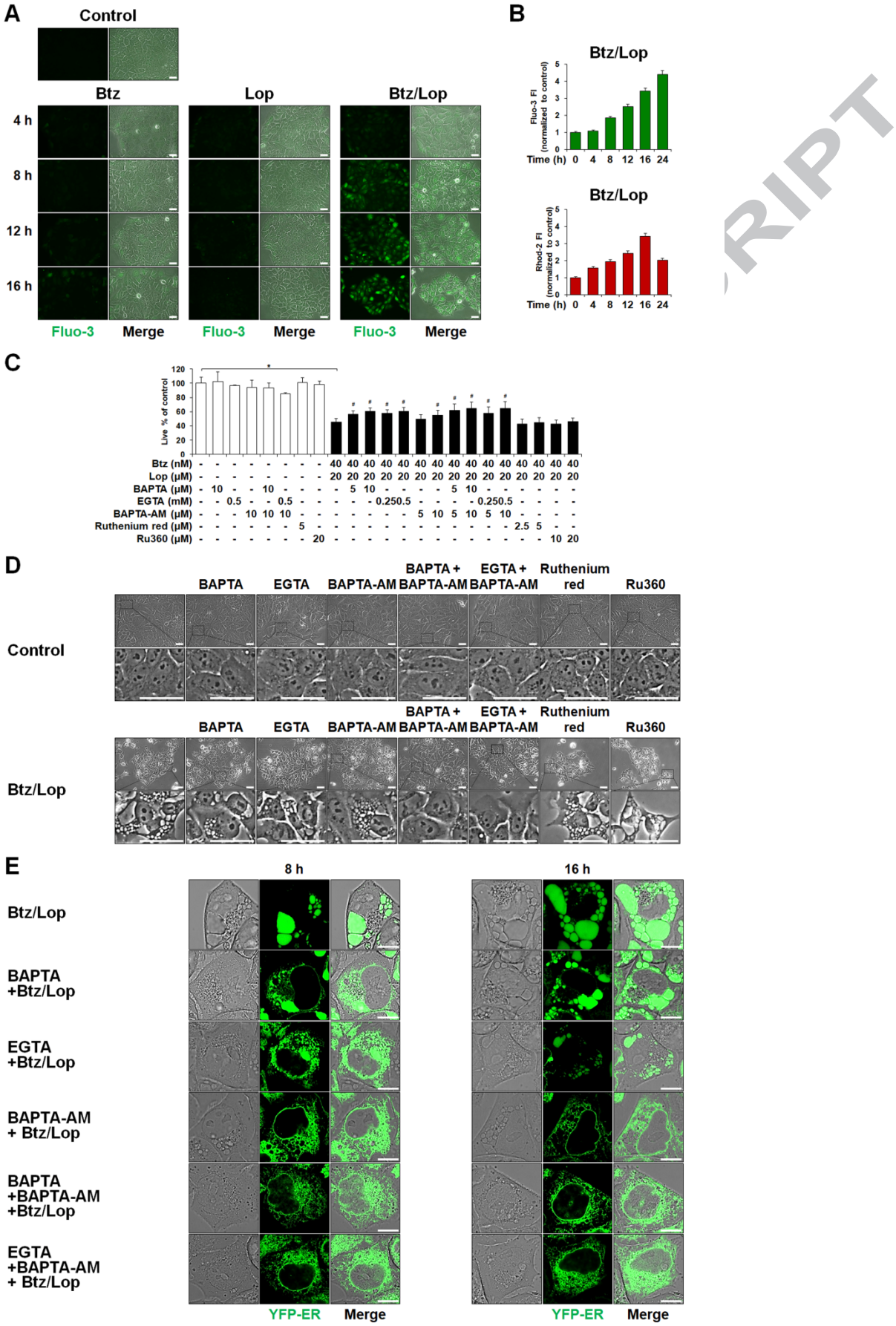

Figure 6. Molecular ordering of key signals involved in Btz/Lop-induced paraptosis-like cell death.

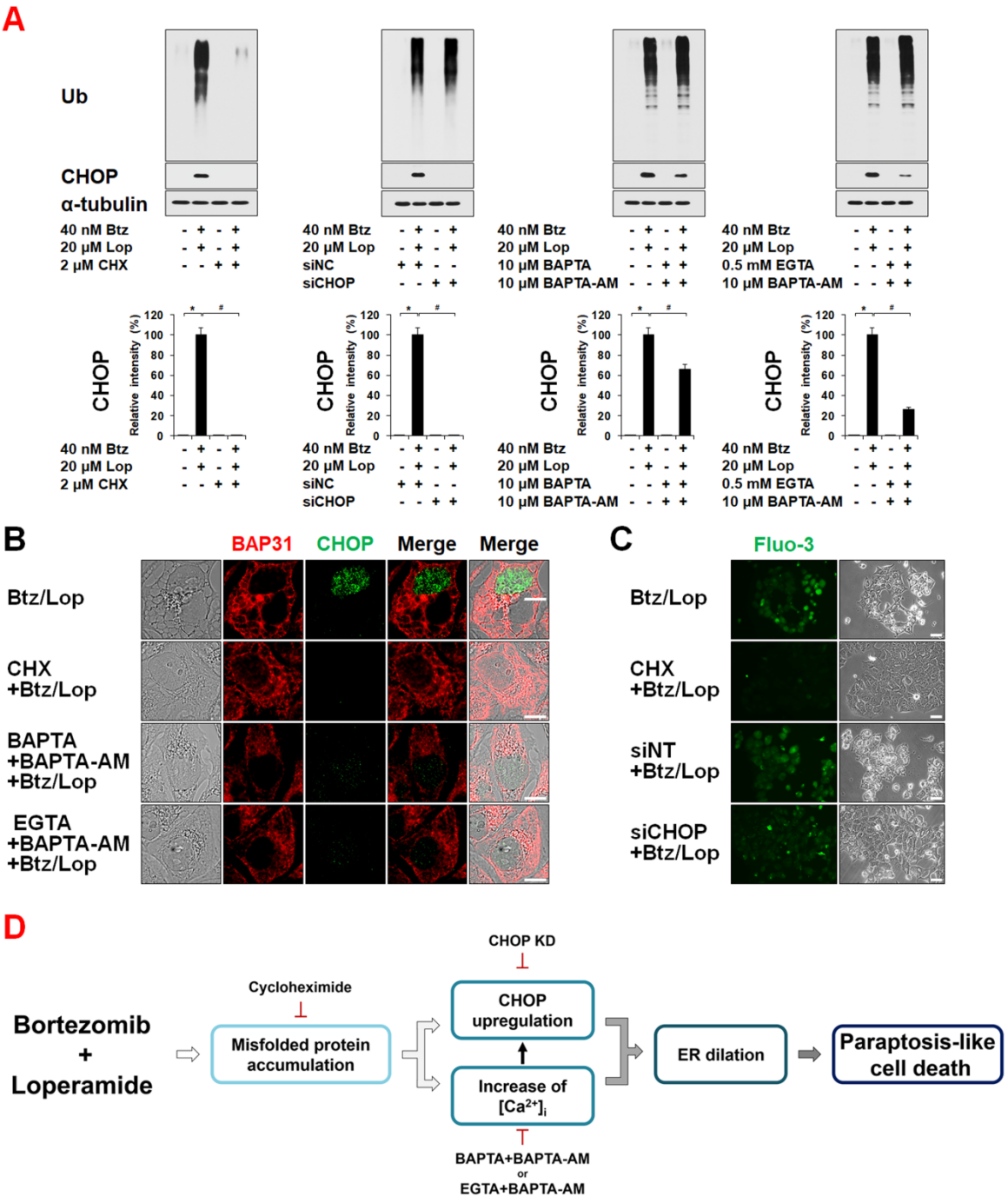

Figure 7. Paraptosis-like cell death accompanied by ER stress and ER dilation is not induced in normal colon cells treated with Btz/Lop.